

Pinning Synchronization for Stochastic Complex Networks With Randomly Occurring Nonlinearities: Tackling Bit Rate Constraints and Allocations

Yuru Guo, Zidong Wang, *Fellow, IEEE*, Jun-Yi Li, *Member, IEEE*, and Yong Xu, *Member, IEEE*

Abstract—In this paper, the ultimately bounded synchronization problem is investigated for a class of discrete-time stochastic complex networks under the pinning control strategy. Communication between system nodes and the remote controller is facilitated via wireless networks subject to bit rate constraints. The system model is distinguished by the inclusion of randomly occurring nonlinearities. A coding-decoding transmission mechanism under constrained bit rates is introduced to characterize the digital transmission process. To achieve synchronization of the network nodes with the unforced target node, a pinning controller is specifically devised based on the information from partially selected nodes. Through the application of the stochastic analysis method, a sufficient condition is derived for ensuring the mean-square boundedness of the synchronization error system. In addition, an optimization algorithm is introduced to address bit rate allocation and the design of desired controller gains. Within the presented theoretical framework, the correlation between the mean-square synchronization performance and bit rate allocation is further elucidated. To conclude, a simulation example is provided to substantiate the efficacy of the recommended pinning control approach.

Index Terms—Stochastic complex networks, bit rate constraint, pinning control, synchronization, randomly occurring nonlinearities.

I. INTRODUCTION

Complex networks (CNs), comprised of numerous interconnected nodes, represent a class of dynamical systems marked by significant complexity [21]. Owing to their adeptness in modeling large-scale complex systems, CNs have been applied extensively in diverse real-world contexts, including transportation networks, social networks, power grids, and biological networks [2], [4]–[6], [9], [32]. The dynamic nodes

This work was supported in part by the Natural Science Foundation of Guangdong Province of China under Grants 2021B0101410005, 2021A1515011634 and 2021B1515420008, the National Natural Science Foundation of China under Grants U22A2044 and 62206063, the Key Area Research and Development Program of Guangdong Province of China under Grant 2021B0101410005, the Local Innovative and Research Teams Project of Guangdong Special Support Program of China under Grant 2019BT02X353, and the China Scholarship Council under Grant 202208440312. (*Corresponding author: Jun-Yi Li*)

Yuru Guo, Jun-Yi Li and Yong Xu are with the Guangdong-Hong Kong Joint Laboratory for Intelligent Decision and Cooperative Control, Guangdong Provincial Key Laboratory of Intelligent Decision and Cooperative Control, School of Automation, Guangdong University of Technology, Guangzhou 510006, China. Jun-Yi Li is also with the Pazhou Lab, Guangzhou 510330, China. (E-mails: guo_yuru0626@163.com; jun-yi-li@foxmail.com; yxu@gdut.edu.cn)

Zidong Wang is with the Department of Computer Science, Brunel University London, Uxbridge UB8 3PH, United Kingdom. (E-mail: Zidong.Wang@brunel.ac.uk)

within CNs interact based on a specific topological structure, thereby establishing a profoundly interconnected network environment. To date, studies on CNs, which encompass stability analysis, synchronization control, and state estimation, have garnered escalating scholarly attention [24], [47], [50], [52].

In practical engineering applications, CNs frequently encounter stochastic perturbations that predominantly arise from the stochastic fluctuations of network parameters [37], [40]. Such inherent stochasticity largely affects the network's overall behavior, which leads to heightened interest in stochastic complex networks (SCNs) and numerous studies being published on the subject [16], [41]. For instance, in [18], stochastic delays in measurement outputs have been modeled using a set of stochastic variables with established probability distributions, and the state estimation issue has been addressed. Similarly, in [7], synchronization within SCNs has been explored by representing the consecutive packet loss phenomenon through specific stochastic variables. It is noteworthy that the aforementioned studies have predominantly focused on SCNs where stochasticity manifests during data transmission processes (e.g. stochastic packet dropouts). Nevertheless, other real-world SCNs often manifest stochastic characteristics in various aspects, such as system structure, node connections, mode transitions, and coupling intensity [33]. Investigating randomly occurring nonlinearities caused by abrupt parameter switches and environmental fluctuations is particularly significant in practical scenarios.

Synchronization is a pivotal concern in CNs with the objective of achieving a unified network behavior, which ensures that node states converge into a consistent pattern or rhythm [42], [46]. The significance of synchronization is evident across a variety of sectors such as communication systems [29], robot systems [22], and neural networks, among others. Synchronization can be categorized based on specific criteria, yielding types like complete synchronization, cluster synchronization [49], bounded synchronization [51], and finite-time synchronization [12], [39]. Notably, bounded synchronization focuses on limiting the disparities in states among network nodes to a specific boundary range, especially when confronted with bounded perturbations. It is imperative to note that bounded synchronization, in comparison to complete synchronization, offers enhanced resilience to faults or disturbances, rendering it an efficacious strategy for addressing SCNs.

The development of suitable control strategies serves as a potent means to enhance the synchronization of CNs.

Among the myriad of control methodologies available, pinning control emerges as a particularly resource-efficient and effective control mechanism [15], [34]. Central to pinning control is the tactic of judiciously selecting a subset of pivotal nodes to which control signals are applied. The remaining nodes, in turn, adhere to their inherent dynamics or liaise with their neighbors, and this ensures that the network as a whole gravitates towards synchronization [48]. In contrast to the traditional global control strategy [43], pinning control boasts advantages in terms of flexibility, cost-efficiency, and scalability. It is a highly promising avenue for application, especially in scenarios where network resources are limited.

It is worth highlighting that the majority of the extant synchronization control strategies have been tailored for continuous-time CNs operating within analog communication frameworks. However, the swift advancements in digital network technology have instigated a paradigm shift in control systems. Traditional analog communication no longer suffices in catering to the communication demands of contemporary control systems. Digital communication strategies, exhibiting merits such as enhanced robustness, reliability, and reduced power consumption, have appeared as a more advantageous alternative [14], [23], [25], [28], [44]. Currently, there is a limited body of research addressing control challenges in CNs over digital communication networks. For instance, in [20], the stabilization issues have been investigated for event-triggered systems operating under bandwidth-restricted networks. Meanwhile, an encryption-decryption framework has been introduced in [13] for cyber-physical systems within the digital network framework.

In wireless digital networks, the coding-decoding process is crucial to data transmissions between devices, which facilitates the transformation of analog signals into digital forms through a sequence of operations including sampling, quantization, and coding, allowing for efficient transmission across digital channels [1], [35], [45]. During the sampling and quantization phases, analog signals are discretized, and these discrete versions are subsequently transformed into codewords composed of binary values, specifically 0 and 1, via the coding step. During decoding, the acquired digital data is reverted back to its analog form. For theoretical analysis, it is necessary to incorporate the coding-decoding framework when evaluating a networked control system, since the coding-decoding operation shapes the nature of the signal received by devices and profoundly influences system behaviors.

In the realm of digital communication networks, bandwidth limitation is an inherent challenge that can culminate in undesirable outcomes such as signal fadings and packet dropouts, especially when there is a need to transmit a vast amount of data concurrently [26], [36]. A fundamental metric for assessing network bandwidth is the bit rate, which delineates the volume of data that can be relayed through digital communication networks within a given time unit. Practically speaking, due to limited bandwidth resources, the rate at which networks transmit information is restricted. Using constrained bit rates as a representation of limited bandwidth, according to the definition of bit rate, is an intuitive approach. Nevertheless, this poses significant hurdles to guaranteeing fast and reliable data

transmission in wireless digital networks. While there have been preliminary studies addressing the control challenge in the context of bit rate limitations for CNs [3], [8], [10], [17], [27], [31], the specific issue of pinning synchronization for discrete-time SCNs under such constraints remains relatively unexplored, even though it holds considerable theoretical and practical implications.

To recap the discussions thus far, our primary focus is on addressing the pinning synchronization issue for SCNs especially in the presence of bit rate constraints and random nonlinearities. In doing so, we are confronted with three predominant challenges: 1) how can we formulate a holistic mathematical model that aptly encapsulates both the stochastic nature of CNs and the bit rate limitations inherent in the communication network? 2) how to design control strategies to adapt to communication-constrained networks and effectively achieve SCNs synchronization? 3) what approach should we employ to analyze the relationship between constrained bit rate and synchronization performance? and 4) what strategies can be devised to optimize the synchronization performance, albeit with constraints on the overall available bit rate of the network?

In response to the aforementioned challenges, our key contributions can be succinctly encapsulated as follows.

- 1) The exploration of the discrete-time synchronization challenge is carried out for SCNs with randomly occurring nonlinearities, specifically within the context of digital communication networks, where the inherent bandwidth limitations are characterized by the bit rate constraints.
- 2) A pinning control strategy is applied, for the first time, to the synchronization of SCNs under constrained bit rates. Due to its characteristic of requiring only a subset of nodes to transmit data within the network, pinning control strategy is particularly suitable for wireless network with limited bandwidth.
- 3) Furthermore, a sufficient condition is established to ensure the mean-square boundedness of the synchronization error dynamics (SED). The relationship between synchronization performance and bit rate allocation is characterized, as reflected in the upper bound of the error.
- 4) An innovative methodology is proposed that aims at enhancing synchronization performance, and such a methodology includes a cooperative optimization algorithm dedicated to bit rate allocation paired with the design of controller gains.

The structure of this paper is laid out as follows. In Section II, we establish the comprehensive models of SCNs featuring random nonlinearities, outline the coding-decoding process, discuss the employed pinning controller, and subsequently detail the ensuing SED. Section III showcases the crux of our findings, encompassing the boundedness analysis, the controller gain design, and the co-design of bit rate allocation strategy and controller gains. In Section IV, we offer a numerical example, complemented by discussions, to affirm the validity of our theoretical conclusions. We draw our

discussions to a close in Section V with concluding remarks.

Notations: Throughout this article, various symbols are employed for mathematical clarity. \mathbb{R}^m denotes the m -dimensional Euclidean space. $\mathbb{R}^{m \times n}$ refers to the set of $m \times n$ real matrices. \mathbb{R} and \mathbb{N} represent the set of all real numbers and non-negative integers, respectively. The Euclidean norm is depicted by $\|\cdot\|_2$, and the absolute value is represented by $|\cdot|$. The symbols \setminus and $*$ signify, respectively, the difference set and the symmetric part of the matrix. Expectation of a stochastic variable is given by $\mathbb{E}\cdot$. For any matrix X , its transpose is expressed as X^T , its trace is signified by $\text{tr}(X)$, and $\lambda_{\max}(X)$ and $\lambda_{\min}(X)$ respectively denote its maximum and minimum eigenvalues. $\text{col}_N \cdot$ is used to denote a column vector comprised of N identical elements. The diagonal matrix is articulated as $\text{diag}\cdot\cdot\cdot$. The Kronecker product is represented by the symbol \otimes . I_n stands for the identity matrix of dimension n . $x \sim \mathbb{U}\{a, b\}$ represents that the element of vector x is a random variable uniformly distributed over the integers from a to b .

II. PROBLEM FORMULATION AND PRELIMINARIES

A. Stochastic Nonlinear Complex Networks

We consider a class of SCNs with randomly occurring nonlinearities represented by

$$\begin{aligned} x_i(s+1) = & Ax_i(s) + \gamma(s)Bf(x_i(s)) + (1 - \gamma(s)) \\ & \times Dg(x_i(s)) + \sum_{j=1}^N \omega_{ij}\Gamma x_j(s) + M_i\theta(s) \\ & + u_i(s), \quad i \in F \triangleq \{1, 2, \dots, N\} \end{aligned} \quad (1)$$

where $x_i(s) \triangleq [x_{i,1}(s) \ x_{i,2}(s) \ \dots \ x_{i,j}(s)] \in \mathbb{R}^n$ and $u_i(s) \in \mathbb{R}^n$ denote the state vector and the control input of SCNs, respectively; $\theta(s) \in \mathbb{R}^v$ is the stochastic noise with zero mean and known variance $\Theta > 0$; $f(x_i(s)) \in \mathbb{R}^n$ and $g(x_i(s)) \triangleq [g_1(x_{i,1}(s)) \ \dots \ g_n(x_{i,n}(s))]^T \in \mathbb{R}^n$ are two kinds of nonlinear functions that will be introduced later; A , B , D , and M_i are known matrices; the inner coupling matrix $\Gamma \triangleq \text{diag}\{r_1, r_2, \dots, r_n\}$ represents the relationship between each element of different nodes' state, and $r_j \neq 0$ ($j = 1, 2, \dots, n$) means that the j -th element of the state of node j has an effect on node i ; the coupled configuration matrix $W \triangleq \{\omega_{ij}\} \in \mathbb{R}^{n \times n}$ satisfies $\sum_{j=1}^N \omega_{ij} = 0$ ($i \in F$), and node j can receive signals from node i if $\omega_{ij} > 0$, otherwise, $\omega_{ij} = 0$.

A Bernoulli random variable sequence $\gamma(s)$ is used to describe the random switching of different nonlinearities, which has the following properties:

$$\mathbb{E}\{\gamma(s)\} = \alpha, \quad \mathbb{E}\{(\gamma(s) - \alpha)^2\} = o^2$$

where α and o are two known constants.

The SCNs experience the nonlinearity $f(\cdot)$ when $\gamma(s) = 1$ and the nonlinearity $g(\cdot)$ when $\gamma(s) = 0$. The nonlinear functions $f(x_i(s))$ and $g(x_i(s))$ satisfy the following assumptions, respectively.

Assumption 1: For any vectors $z_1 \in \mathbb{R}^n$ and $z_2 \in \mathbb{R}^n$, the nonlinearity $f(\cdot)$ with $f(0) = 0$ satisfies the following condition:

$$\|f(z_1) - f(z_2) - \chi(z_1 - z_2)\|_2 \leq \rho\|z_1 - z_2\|_2$$

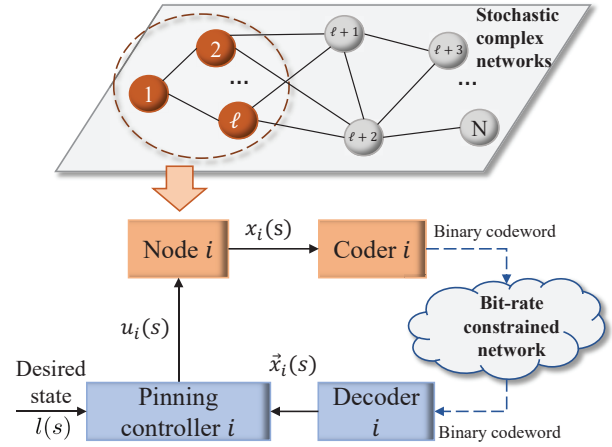


Fig. 1. Schematic of synchronization under constrained bit rate.

where $\chi \in \mathbb{R}^{n \times n}$ is a known matrix and ρ is a known nonnegative scalar.

Assumption 2: For any scalars $m_1, m_2 \in \mathbb{R}$ ($m_1 \neq m_2$), the nonlinear function $g_j(\cdot) \in \mathbb{R}$ ($\forall j \in \{1, 2, \dots, n\}$) satisfies $g_j(0) = 0$ and

$$\underline{\tau}_j \leq \frac{g_j(m_1) - g_j(m_2)}{m_1 - m_2} \leq \bar{\tau}_j$$

where $\underline{\tau}_j$ and $\bar{\tau}_j$ are two known constants.

B. Coding-Decoding Procedure Under Constrained Bit Rate

In practical scenarios, the bandwidth of wireless communication networks is often limited, signifying a restriction on the number of bits that can be transmitted at each sampling instant. As depicted in Fig. 1, the pinning control strategy is employed on the considered SCNs with the aim of conserving network resources and reducing control costs. Under this strategy, only a subset of nodes in the SCNs is selected to convey information to their corresponding controllers. Without loss of generality, we assume that the first ℓ nodes in the set F are designated for data transmissions, and the remaining $N - \ell$ nodes do not utilize the network for data transmission. For clarity, the set of nodes chosen for data transmissions is represented by $F_0 \triangleq \{1, 2, \dots, \ell\}$.

For a communication network with a constrained bit rate, appropriate bit rate allocation for each selected node becomes imperative. Let's assume that the total number of available bits for the entire wireless network is represented by U ($U \in \mathbb{N}$). Consequently, the bit rate U_i allocated to node i complies with the following condition [11]:

$$U \geq \sum_{i=1}^{\ell} U_i, \quad U_i \in \mathbb{N}, \quad (2)$$

which means that each coder has limited bit rate to encode the data packet. As a result, data compression becomes essential, which can be realized using a uniform quantizer. Specifically, this quantizer segments the quantization region into a set number of uniformly spaced intervals. The quantization procedure entails associating each input data point with its corresponding

interval. Assuming that the quantization level for node i is represented by q_i (denoting the number of intervals), it is necessary to describe q_i^n mapping cases with U_i bits for the state $x_i(s)$ with n elements. The maximum quantization level \hat{q}_i adheres to the following condition:

$$\hat{q}_i \triangleq \lfloor \sqrt[n]{2^{U_i}} \rfloor, \quad i \in F_0 \quad (3)$$

where the symbol $\lfloor \cdot \rfloor$ stands for rounding down function.

Given a scalar $\delta_i > 0$ representing the upper bound of the quantization region, the following holds:

$$|x_{i,j}(s)| \leq \delta_i, \quad \forall j \in \{1, 2, \dots, n\}, \quad i \in F_0. \quad (4)$$

With the quantization level q_i , the quantization region for node i is uniformly divided into the following sub-hyperrectangles:

$$\begin{aligned} \mathcal{Q}_{i,j}^{(1)}(\delta_i) &\triangleq \left\{ x_{i,j}(s) \mid -\delta_i \leq x_{i,j}(s) < -\delta_i + \frac{2\delta_i}{q_i} \right\} \\ \mathcal{Q}_{i,j}^{(2)}(\delta_i) &\triangleq \left\{ x_{i,j}(s) \mid -\delta_i + \frac{2\delta_i}{q_i} \leq x_{i,j}(s) < -\delta_i + \frac{4\delta_i}{q_i} \right\} \\ &\vdots \\ \mathcal{Q}_{i,j}^{(q_i)}(\delta_i) &\triangleq \left\{ x_{i,j}(s) \mid \delta_i - \frac{2\delta_i}{q_i} \leq x_{i,j}(s) \leq \delta_i \right\}. \end{aligned} \quad (5)$$

To facilitate the binary representation of state information, the quantization region corresponding to each element of node i is denoted by a string of integers $\{d_{i,1}, d_{i,2}, \dots, d_{i,n}\} \in \{1, 2, \dots, q_i\}$. The coder i encodes this string of integers using binary representation 0 and 1, and then outputs the binary codeword $\tilde{X}_i(s) \triangleq \aleph(\{d_{i,1}, d_{i,2}, \dots, d_{i,n}\})$, where $\aleph(\cdot)$ denotes the coding function. Subsequently, the binary codeword $\tilde{X}_i(s)$ will be transmitted to the decoder i over the wireless communication network by utilizing the same transmission protocol according to coder i . After decoding, the central values $\{\varrho_{i,1}, \varrho_{i,2}, \dots, \varrho_{i,n}\}$ of the sub-hyperrectangles are used to approximate the original data, which is computed by

$$\varrho_{i,j} = -\delta_i + \frac{(2d_{i,j} - 1)\delta_i}{q_i}, \quad j \in \{1, 2, \dots, n\}. \quad (6)$$

Based on the above analysis, the quantization error of the state $x_i(s)$ satisfies

$$\left\| x_i(s) - [\varrho_{i,1} \quad \varrho_{i,2} \quad \dots \quad \varrho_{i,n}]^T \right\|_2 \leq \frac{\sqrt{n}\delta_i}{q_i}. \quad (7)$$

Denote the decoding output as $\vec{x}_i(s) \triangleq [\varrho_{i,1} \quad \varrho_{i,2} \quad \dots \quad \varrho_{i,n}]^T$. Then, the decoding error is obtained as follows

$$\psi_i(s) \triangleq x_i(s) - \vec{x}_i(s). \quad (8)$$

Remark 1: In wireless communication networks, bit rate allocation often adheres to specific communication standards or protocols. There are two prevalent methods: the dynamic bit rate adjustment protocol and the allocation-based static bit rate protocol. The former dynamically allocates fluctuating bit rates to user devices, optimizing data transmission efficiency based on individual needs. In contrast, the latter ensures

equitable data transmission opportunities and is particularly apt for situations where multiple users share limited bandwidth resources. In this study, the static bit rate allocation protocol is employed for the SCNs.

C. Pinning Controller for Bit-Rate Constrained Network

In the context of CNs, pinning control is a method that ensures synchronization or stabilization by implementing control laws to a select set of nodes, termed as ‘‘pinned nodes’’. By adhering to the principles of pinning control, the pinned nodes that are chosen in this study belong to the set F_0 defined in Section II-B. The primary aim of this research is to ensure synchronization between nodes within the SCNs and a target node which is not subjected to any external forces, and this is done via the design of the pinning controller. More specifically, only the nodes that are part of the set F_0 are affected by the designed control laws. Meanwhile, the other nodes in the SCNs progress based on their interconnected dynamics with the pinned nodes. The ultimate goal is to ensure that all nodes synchronize effectively.

The unforced target node is modeled as follows:

$$\begin{aligned} l(s+1) &= Al(s) + \alpha Bf(l(s)) \\ &\quad + (1 - \alpha)Dg(l(s)) + u_0(l(s)) \end{aligned} \quad (9)$$

where $l(s) \in \mathbb{R}^n$ is the state of the target node, and $u_0(l(s)) \in \mathbb{R}^n$ is the control input satisfying the following Lipschitz condition:

$$\|u_0(y_1) - u_0(y_2)\|_2 \leq L\|y_1 - y_2\|_2 \quad (10)$$

where L is a Lipschitz constant, and $y_1, y_2 \in \mathbb{R}^n$ are any vectors with $u_0(0) = 0$. By the control input $u_0(l(s))$, the desired dynamical behavior of state $l(s)$ is guaranteed. We suppose that there exist a positive constant \bar{l} and time instant $T(0)$ such that, for any initial condition $l(0)$, $\|l(s)\|_2 \leq \bar{l}$ holds for $\forall s \geq T(0)$ [19].

We adopt the following pinning synchronization controller:

$$u_i(s) = \begin{cases} K_i(\vec{x}_i(s) - l(s)), & i \in F_0 \\ 0, & i \in F \setminus F_0 \end{cases} \quad (11)$$

where K_i denotes the controller gain to be designed.

By combining (1) with (11), the closed-loop SCNs are obtained as follows:

$$\begin{cases} x_i(s+1) = Ax_i(s) + \gamma(s)Bf(x_i(s)) + (1 - \gamma(s)) \\ \quad \times Dg(x_i(s)) + \sum_{j=1}^N \omega_{ij}\Gamma x_j(s) \\ \quad + M_i\theta(s) + K_i(\vec{x}_i(s) - l(s)), \quad i \in F_0 \\ x_i(s+1) = Ax_i(s) + \gamma(s)Bf(x_i(s)) + (1 - \gamma(s)) \\ \quad \times Dg(x_i(s)) + \sum_{j=1}^N \omega_{ij}\Gamma x_j(s) \\ \quad + M_i\theta(s), \quad i \in F \setminus F_0. \end{cases} \quad (12)$$

Remark 2: In the presence of bandwidth constraints, attempting to transmit large volumes of information simultaneously can result in data collisions. However, the beauty

of the pinning control technique used in this study lies in its selectivity. Instead of relying on information from every node, the pinning controller gathers data only from a carefully chosen subset of nodes to bring about synchronization in the entire CNs. This targeted approach considerably reduces the transmission burden on the wireless network, making it an ideal solution for CNs operating under tight bit rate restrictions.

D. Synchronization Error Dynamics

Define $e_i(s) \triangleq x_i(s) - l(s)$ as the synchronization error. By combining (9) with (12), for the controlled nodes, we have that

$$\begin{aligned} e_i(s+1) &= Ae_i(s) + \gamma(s)Bf(x_i(s)) - \alpha Bf(l(s)) \\ &\quad + M_i\theta(s) + (1 - \gamma(s))Dg(x_i(s)) \\ &\quad - (1 - \alpha)Dg(l(s)) + \sum_{j=1}^N \omega_{ij}\Gamma e_j(s) \\ &\quad + K_i(e_i(s) - \psi_i(s)) - u_0(l(s)) \\ &= (A + K_i)e_i(s) + (\gamma(s) - \alpha)B\tilde{f}(e_i(s)) \\ &\quad + \alpha B\tilde{f}(e_i(s)) + (\gamma(s) - \alpha)Bf(l(s)) \\ &\quad - (\gamma(s) - \alpha)D\tilde{g}(e_i(s)) + \sum_{j=1}^N \omega_{ij}\Gamma e_j(s) \\ &\quad + (1 - \alpha)D\tilde{g}(e_i(s)) - (\gamma(s) - \alpha)Dg(l(s)) \\ &\quad - K_i\psi_i(s) + M_i\theta(s) - u_0(l(s)), \quad i \in F_0. \end{aligned} \quad (13)$$

Similarly, for the remaining uncontrolled nodes $i \in F \setminus F_0$, we have

$$\begin{aligned} e_i(s+1) &= Ae_i(s) + (\gamma(s) - \alpha)B\tilde{f}(e_i(s)) + \alpha B\tilde{f}(e_i(s)) \\ &\quad + (\gamma(s) - \alpha)Bf(l(s)) + (1 - \alpha)D\tilde{g}(e_i(s)) \\ &\quad - (\gamma(s) - \alpha)D\tilde{g}(e_i(s)) - (\gamma(s) - \alpha)Dg(l(s)) \\ &\quad + \sum_{j=1}^N \omega_{ij}\Gamma e_j(s) + M_i\theta(s) - u_0(l(s)) \end{aligned} \quad (14)$$

where $\tilde{f}(e_i(s)) \triangleq f(x_i(s)) - f(l(s))$ and $\tilde{g}(e_i(s)) \triangleq g(x_i(s)) - g(l(s))$.

Define the augmented error vector as $e(s) \triangleq [e_1^T(s) \ e_2^T(s) \ \dots \ e_N^T(s)]^T$. Then, we further have

$$\begin{aligned} e(s+1) &= \Lambda e(s) + (\gamma(s) - \alpha)\hat{B}\tilde{\mathcal{F}}(e(s)) + \alpha\hat{B}\tilde{\mathcal{F}}(e(s)) \\ &\quad + (\gamma(s) - \alpha)\hat{B}\mathcal{F}(l(s)) - (\gamma(s) - \alpha)\hat{D}\tilde{\mathcal{G}}(e(s)) \\ &\quad + (1 - \alpha)\hat{D}\tilde{\mathcal{G}}(e(s)) - (\gamma(s) - \alpha)\hat{D}\mathcal{G}(l(s)) \\ &\quad + M\theta(s) - \tilde{K}\Phi(s) - \mathcal{U}_0(s) \end{aligned} \quad (15)$$

where

$$\begin{aligned} \Lambda &\triangleq \hat{A} + W \otimes \Gamma + \tilde{K}, \quad \hat{A} \triangleq I_N \otimes A, \\ \mathcal{U}_0(s) &\triangleq \text{col}_N\{u_0(l(s))\}, \quad \hat{B} \triangleq I_N \otimes B, \\ \hat{D} &\triangleq I_N \otimes D, \quad M \triangleq [M_1^T \ M_2^T \ \dots \ M_N^T]^T, \\ \Phi(s) &\triangleq [\psi_1^T(s) \ \psi_2^T(s) \ \dots \ \psi_N^T(s)]^T, \\ \tilde{\mathcal{F}}(e(s)) &\triangleq [\tilde{f}^T(e_1(s)) \ \tilde{f}^T(e_2(s)) \ \dots \ \tilde{f}^T(e_N(s))]^T, \\ \tilde{\mathcal{G}}(e(s)) &\triangleq [\tilde{g}^T(e_1(s)) \ \tilde{g}^T(e_2(s)) \ \dots \ \tilde{g}^T(e_N(s))]^T, \end{aligned}$$

$$\begin{aligned} \mathcal{F}(l(s)) &\triangleq \text{col}_N\{f(l(s))\}, \quad \mathcal{G}(l(s)) \triangleq \text{col}_N\{g(l(s))\}, \\ \tilde{K} &\triangleq \text{diag}\{K, 0\}, \quad K \triangleq \text{diag}\{K_1, K_2, \dots, K_\ell\}. \end{aligned}$$

The following lemma and definition are introduced to facilitate later analysis.

Lemma 1: [30] For any vectors $d \in \mathbb{R}^n$ and $h \in \mathbb{R}^n$, and a positive definite matrix $Q \in \mathbb{R}^{n \times n}$, the following relationship holds:

$$2d^T h \leq d^T Q d + h^T Q^{-1} h. \quad (16)$$

Definition 1: [38] The SED (15) is said to be exponentially mean-square bounded, if there exist constants $|a| < 1$, $b > 0$ and $c > 0$ such that the following inequality holds:

$$\mathbb{E}\{\|e(s)\|_2^2\} \leq a^s b + c \quad (17)$$

where c is the asymptotic upper bound (AUB) of $\mathbb{E}\{\|e(s)\|_2^2\}$.

III. MAIN RESULTS

In this section, an analysis of the mean-square boundedness for the SED is presented. Subsequently, the pinning controller is formulated considering specified bit rates and an optimized allocation protocol.

A. Boundedness Analysis

In the following theorem, a sufficient condition is given to discuss the exponential boundedness in the mean-square sense of the SED.

Theorem 1: Consider the SCNs (1), the target node (9), and the pinning controller (11) with given positive integers U , U_i , and controller gain matrices K_i ($i \in F_0$). Then, the SED (15) is exponentially mean-square bounded if there exist positive scalars $0 < \beta_1 < 1$, β_2 , β_3 , ε_1 , ε_2 , and positive definite matrices \tilde{P}_i ($i \in F$), Q_1 and Q_2 such that the following inequality holds:

$$\begin{bmatrix} \Omega_{11} & \Omega_{12} & \Omega_{13} & \Omega_{14} & \Omega_{15} \\ * & -P^{-1} & 0 & 0 & 0 \\ * & * & -P^{-1} & 0 & 0 \\ * & * & * & -Q_1 & 0 \\ * & * & * & * & -Q_2 \end{bmatrix} < 0 \quad (18)$$

where

$$\Omega_{11} \triangleq \begin{bmatrix} \hat{\Omega}_{111} & \bar{\chi}^T & -\Xi_{13} & 0 & 0 \\ * & -\varepsilon_1 I_{nN} & 0 & 0 & 0 \\ * & * & -\varepsilon_2 I_{nN} & 0 & 0 \\ * & * & * & -\beta_2 I_{nN} & 0 \\ * & * & * & * & -\beta_3 I_{nN} \end{bmatrix},$$

$$\hat{\Omega}_{111} \triangleq (\beta_1 - 1)P - \Xi_{11},$$

$$\Omega_{12} \triangleq [\Lambda \quad \alpha\hat{B} \quad (1 - \alpha)\hat{D} \quad -\tilde{K} \quad -I_{nN}]^T,$$

$$\Omega_{13} \triangleq [0 \quad o\hat{B} \quad -o\hat{D} \quad 0 \quad 0]^T,$$

$$\Omega_{14} \triangleq [0 \quad oP^T\hat{B} \quad 0 \quad 0 \quad 0]^T,$$

$$\Omega_{15} \triangleq [0 \quad 0 \quad oP^T\hat{D} \quad 0 \quad 0]^T,$$

$$\Xi_{11} \triangleq \varepsilon_1 \bar{\chi}^T \bar{\chi} - \varepsilon_1 \rho^2 I_{nN} + \varepsilon_2 \Upsilon_1^T \Upsilon_2,$$

$$\begin{aligned}\Xi_{13} &\triangleq -\varepsilon_2(\Upsilon_1^T + \Upsilon_2^T)/2, \quad \bar{\chi} \triangleq I_N \otimes \chi, \\ \Upsilon_1 &\triangleq I_N \otimes \text{diag}\{\underline{\tau}_1, \underline{\tau}_2, \dots, \underline{\tau}_n\}, \\ \Upsilon_2 &\triangleq I_N \otimes \text{diag}\{\bar{\tau}_1, \bar{\tau}_2, \dots, \bar{\tau}_n\}, \\ P &\triangleq \text{diag}\{\tilde{P}_1, \tilde{P}_2, \dots, \tilde{P}_N\}.\end{aligned}$$

Proof 1: Choose the following Lyapunov-like function for boundedness analysis:

$$V(s) = e^T(s)Pe(s). \quad (19)$$

Calculating the mathematical expectation of the difference of $V(s)$, one has

$$\begin{aligned}\Delta V(s) &\triangleq \mathbb{E}\{V(s+1)|V(s)\} - V(s) \\ &= e^T(s)\Lambda^T P \Lambda e(s) + (o^2 + \alpha^2)\tilde{\mathcal{F}}^T(e(s))\hat{B}^T P \hat{B} \\ &\quad \times \tilde{\mathcal{F}}(e(s)) + (o^2 + (1-\alpha)^2)\tilde{\mathcal{G}}^T(e(s))\hat{D}^T P \hat{D} \\ &\quad \times \tilde{\mathcal{G}}(e(s)) + \Phi^T(s)\tilde{K}^T P \tilde{K} \Phi(s) + 2o^2\tilde{\mathcal{F}}^T(e(s)) \\ &\quad \times \hat{B}^T P H(s) + o^2 H^T(s) P H(s) + 2\alpha e^T(s)\Lambda^T \\ &\quad \times P \hat{B} \tilde{\mathcal{F}}(e(s)) + 2(1-\alpha)e^T(s)\Lambda^T P \hat{D} \tilde{\mathcal{G}}(e(s)) \\ &\quad - 2e^T(s)\Lambda^T P \tilde{K} \Phi(s) - 2o^2\tilde{\mathcal{F}}^T(e(s))\hat{B}^T P \hat{D} \tilde{\mathcal{G}}(e(s)) \\ &\quad + \mathbb{E}\{\theta^T(s)M^T P M \theta(s)\} + 2\alpha(1-\alpha)\tilde{\mathcal{F}}^T(e(s)) \\ &\quad \times \hat{B}^T P \hat{D} \tilde{\mathcal{G}}(e(s)) - e^T(s)Pe(s) - 2\tilde{\mathcal{F}}^T(e(s)) \\ &\quad \times \hat{B}^T P \tilde{K} \Phi(s) - 2o^2\tilde{\mathcal{G}}^T(e(s))\hat{D}^T P H(s) \\ &\quad - 2(1-\alpha)\tilde{\mathcal{G}}^T(e(s))\hat{D}^T P \tilde{K} \Phi(s) + \mathcal{U}_0^T(s) \\ &\quad \times P \mathcal{U}_0(s) - 2e^T(s)\Lambda^T P \mathcal{U}_0(s) - 2(1-\alpha) \\ &\quad \times \tilde{\mathcal{G}}^T(e(s))\hat{D}^T P \mathcal{U}_0(s) + 2\Phi^T(s)\tilde{K}^T P \mathcal{U}_0(s) \\ &\quad - 2\alpha\tilde{\mathcal{F}}^T(e(s))\hat{B}^T P \mathcal{U}_0(s)\end{aligned} \quad (20)$$

where $H(s) \triangleq \hat{B}\mathcal{F}(l(s)) - \hat{D}\mathcal{G}(l(s))$.

According to Lemma 1, the following inequalities hold:

$$2o^2\tilde{\mathcal{F}}^T(e(s))\hat{B}^T P H(s) \leq o^2 H^T(s)Q_1 H(s) + o^2\tilde{\mathcal{F}}^T(e(s))\hat{B}^T P Q_1^{-1} P^T \hat{B} \tilde{\mathcal{F}}(e(s)), \quad (21)$$

$$2o^2\tilde{\mathcal{G}}^T(e(s))\hat{D}^T P H(s) \leq o^2 H^T(s)Q_2 H(s) + o^2\tilde{\mathcal{G}}^T(e(s))\hat{D}^T P Q_2^{-1} P^T \hat{D} \tilde{\mathcal{G}}(e(s)). \quad (22)$$

Define an augmented vector as

$$\xi(s) \triangleq [e^T(s) \quad \tilde{\mathcal{F}}^T(e(s)) \quad \tilde{\mathcal{G}}^T(e(s)) \quad \Phi^T(s) \quad \mathcal{U}_0^T(s)]^T.$$

Combining (20) with (21) and (22) results in

$$\begin{aligned}\Delta V(s) &\leq \xi^T(s) \begin{bmatrix} \Pi_{11} & \Pi_{12} & \Pi_{13} & \Pi_{14} & \Pi_{15} \\ * & \Pi_{22} & \Pi_{23} & \Pi_{24} & \Pi_{25} \\ * & * & \Pi_{33} & \Pi_{34} & \Pi_{35} \\ * & * & * & \Pi_{44} & \Pi_{45} \\ * & * & * & * & \Pi_{55} \end{bmatrix} \xi(s) \\ &\quad + \mathbb{E}\{\theta^T(s)M^T P M \theta(s)\} + \beta_3 \mathcal{U}_0^T(s)\mathcal{U}_0(s) \\ &\quad - \beta_1 e^T(s)Pe(s) + \beta_2 \Phi^T(s)\Phi(s) \\ &\quad + o^2 H^T(s)(P + Q_1 + Q_2)H(s)\end{aligned} \quad (23)$$

where

$$\Pi_{11} \triangleq \Lambda^T P \Lambda + (\beta_1 - 1)P, \quad \Pi_{12} \triangleq \alpha \Lambda^T P \hat{B},$$

$$\begin{aligned}\Pi_{13} &\triangleq (1-\alpha)\Lambda^T P \hat{D}, \quad \Pi_{14} \triangleq -\Lambda^T P \tilde{K}, \\ \Pi_{22} &\triangleq (o^2 + \alpha^2)\hat{B}^T P \hat{B} + o^2 \hat{B}^T P Q_1^{-1} P^T \hat{B}, \\ \Pi_{23} &\triangleq (-o^2 + \alpha(1-\alpha))\hat{B}^T P \hat{D}, \quad \Pi_{24} \triangleq -\alpha \hat{B}^T P \tilde{K}, \\ \Pi_{33} &\triangleq (o^2 + (1-\alpha)^2)\hat{D}^T P \hat{D} + o^2 \hat{D}^T P Q_2^{-1} P^T \hat{D}, \\ \Pi_{34} &\triangleq (\alpha - 1)\hat{D}^T P \tilde{K}, \quad \Pi_{44} \triangleq \tilde{K}^T P \tilde{K} - \beta_2 I_{nN}, \\ \Pi_{15} &\triangleq -\Lambda^T P, \quad \Pi_{25} \triangleq -\alpha \hat{B}^T P, \quad \Pi_{45} \triangleq \tilde{K}^T P, \\ \Pi_{35} &\triangleq (\alpha - 1)\hat{D}^T P, \quad \Pi_{55} \triangleq P - \beta_3 I_{nN}.\end{aligned}$$

It follows from Assumption 1 that the Lipschitz-type nonlinear function $f(\cdot)$ satisfies

$$\begin{aligned}(\tilde{\mathcal{F}}^T(e(s)) - e^T(s)\bar{\chi}^T) \\ \times (\tilde{\mathcal{F}}(e(s)) - \bar{\chi}e(s)) - \rho^2 e^T(s)e(s) \leq 0,\end{aligned} \quad (24)$$

which can be further expressed as

$$\begin{bmatrix} e(s) \\ \tilde{\mathcal{F}}(e(s)) \end{bmatrix}^T \begin{bmatrix} \varepsilon_1 \bar{\chi}^T \bar{\chi} - \varepsilon_1 \rho^2 I_{nN} & -\bar{\chi}^T \\ * & \varepsilon_1 I_{nN} \end{bmatrix} \begin{bmatrix} e(s) \\ \tilde{\mathcal{F}}(e(s)) \end{bmatrix} \leq 0 \quad (25)$$

where $\varepsilon_1 > 0$ is an extra parameter introduced to enhance the feasibility of the control algorithm to be developed.

Similarly, the following relation can be established based on Assumption 2:

$$(\tilde{\mathcal{G}}(e(s)) - \Upsilon_1 e(s))^T (\tilde{\mathcal{G}}(e(s)) - \Upsilon_2 e(s)) \leq 0, \quad (26)$$

which can be represented by

$$\begin{bmatrix} e(s) \\ \tilde{\mathcal{G}}(e(s)) \end{bmatrix}^T \begin{bmatrix} \varepsilon_2 \Upsilon_1^T \Upsilon_2 & -\varepsilon_2 \frac{\Upsilon_2^T + \Upsilon_1^T}{2} \\ * & \varepsilon_2 I_{nN} \end{bmatrix} \begin{bmatrix} e(s) \\ \tilde{\mathcal{G}}(e(s)) \end{bmatrix} \leq 0 \quad (27)$$

where $\varepsilon_2 > 0$ is another free parameter that is added to enable more freedom in designing the controller.

Substituting (25) and (27) into (23) gives

$$\begin{aligned}\Delta V(s) &\leq -\beta_1 V(s) + \xi^T(s)\tilde{\Pi}\xi(s) + \beta_2 \Phi^T(s)\Phi(s) \\ &\quad + \mathbb{E}\{\theta^T(s)M^T P M \theta(s)\} + \beta_3 \mathcal{U}_0^T(s)\mathcal{U}_0(s) \\ &\quad + o^2 H^T(s)(P + Q_1 + Q_2)H(s)\end{aligned} \quad (28)$$

where

$$\tilde{\Pi} \triangleq \begin{bmatrix} \Pi_{11} - \Xi_{11} & \Pi_{12} + \bar{\chi}^T & \Pi_{13} - \Xi_{13} & \Pi_{14} & \Pi_{15} \\ * & \Pi_{22} - \varepsilon_1 I_{nN} & \Pi_{23} & \Pi_{24} & \Pi_{25} \\ * & * & \Pi_{33} - \varepsilon_2 I_{nN} & \Pi_{34} & \Pi_{35} \\ * & * & * & \Pi_{44} & \Pi_{45} \\ * & * & * & * & \Pi_{55} \end{bmatrix}.$$

Applying the Schur Complement Lemma to inequality (18) in Theorem 1, we have $\tilde{\Pi} < 0$, which implies that

$$\begin{aligned}\Delta V(s) &< -\beta_1 V(s) + \mathbb{E}\{\theta^T(s)M^T P M \theta(s)\} \\ &\quad + o^2 H^T(s)(P + Q_1 + Q_2)H(s) \\ &\quad + \beta_2 \Phi^T(s)\Phi(s) + \beta_3 \mathcal{U}_0^T(s)\mathcal{U}_0(s).\end{aligned} \quad (29)$$

In terms of the definition of noise $\theta(s)$, one obtains

$$\begin{aligned}\mathbb{E}\{\theta^T(s)M^T P M \theta(s)\} \\ = \mathbb{E}\{\text{tr}(M^T P M \theta(s)\theta^T(s))\}\end{aligned}$$

$$= \text{tr} (M^T P M \Theta). \quad (30)$$

Furthermore, Assumption 1 implies that

$$\begin{aligned} & \|f(l(s)) - \chi l(s)\|_2 \leq \rho \|l(s)\|_2 \\ \Rightarrow & (f^T(l(s)) - l^T(s)\chi^T)(f(l(s)) - \chi l(s)) \leq \rho^2 l^T(s)l(s) \\ \Rightarrow & \|f(l(s))\|_2^2 - 2\|f^T(l(s))\chi l(s)\|_2 + \|\chi l(s)\|_2^2 \leq \rho^2 \|l(s)\|_2^2 \\ \Rightarrow & (\|f(l(s))\|_2 - \|\chi l(s)\|_2)^2 \leq \rho^2 \|l(s)\|_2^2 \\ \Rightarrow & \|f(l(s))\|_2 \leq \rho \|l(s)\|_2 + \|\chi l(s)\|_2 \leq (\rho + \|\chi\|_2)\bar{l}, \\ & \text{if } \|f(l(s))\|_2 \geq \|\chi l(s)\|_2, \\ & \text{or } \|f(l(s))\|_2 \geq \|\chi l(s)\|_2 - \rho \|l(s)\|_2, \\ & \text{if } \|f(l(s))\|_2 < \|\chi l(s)\|_2. \end{aligned} \quad (31)$$

According to Assumption 2, the bound of $\|g(l(s))\|_2$ is derived as follows:

$$\begin{aligned} & \|g(l(s))\|_2^2 \\ &= g_1^2(l_1(s)) + g_2^2(l_2(s)) + \dots + g_n^2(l_n(s)) \\ &\leq \max_{j \in \{1, 2, \dots, n\}} \{|\bar{\tau}_j|, |\underline{\tau}_j|\}^2 (l_1^2(s) + l_2^2(s) + \dots + l_n^2(s)) \\ &= \max_{j \in \{1, 2, \dots, n\}} \{|\bar{\tau}_j|, |\underline{\tau}_j|\}^2 \|l(s)\|_2^2 \\ &= \max_{j \in \{1, 2, \dots, n\}} \{|\bar{\tau}_j|, |\underline{\tau}_j|\}^2 \bar{l}^2. \end{aligned} \quad (32)$$

It follows from (30)-(32) that

$$\Delta V(s) < -\beta_1 V(s) + \mu.$$

Taking the mathematical expectation of the above inequality, we obtain

$$\mathbb{E}\{V(s+1) - V(s)\} < -\beta_1 \mathbb{E}\{V(s)\} + \mu \quad (33)$$

where

$$\begin{aligned} \mu &\triangleq \sigma^2 \lambda_{\max}(P + Q_1 + Q_2) \bar{h}^2 + \text{tr} (M^T P M \Theta) \\ &\quad + \beta_2 \sum_{i=1}^{\ell} \frac{n \delta_i^2}{[\sqrt{2} U_i]^2} + \beta_3 N L^2 \bar{l}^2, \\ \bar{h} &\triangleq \|\hat{B}\|_2 \sqrt{N} (\rho + \|\chi\|_2) \bar{l} \\ &\quad + \|\hat{D}\|_2 \sqrt{N} \max_{j \in \{1, 2, \dots, n\}} \{|\bar{\tau}_j|, |\underline{\tau}_j|\} \bar{l}. \end{aligned}$$

We deduce from (33) that

$$\begin{aligned} \mathbb{E}\{V(s)\} &< (1 - \beta_1) \mathbb{E}\{V(s-1)\} + \mu \\ &< (1 - \beta_1)^2 \mathbb{E}\{V(s-2)\} + (1 + (1 - \beta_1)) \mu \\ &< \dots \\ &< (1 - \beta_1)^s \mathbb{E}\{V(0)\} + \mu \sum_{i=0}^{s-1} (1 - \beta_1)^i, \end{aligned} \quad (34)$$

which implies

$$\mathbb{E}\{\|e(s)\|_2^2\} < \frac{(1 - \beta_1)^s \mathbb{E}\{V(0)\}}{\lambda_{\min}(P)} + \frac{\mu \sum_{i=0}^{s-1} (1 - \beta_1)^i}{\lambda_{\min}(P)}. \quad (35)$$

From the above analysis, one knows that the following inequality holds as s goes to infinity:

$$\mathbb{E}\{\|e(s)\|_2^2\} < \frac{\mu}{\beta_1 \lambda_{\min}(P)} \triangleq \tilde{O}. \quad (36)$$

Recalling Definition 1, the SED (15) is exponentially mean-square bounded with the upper bound \tilde{O} , which completes the proof.

Remark 3: Ultimate boundedness serves as a crucial performance criterion for SED. In Theorem 1, a sufficient condition is provided to ensure the ultimate boundedness of SED. Based on the error upper bound shown in (36), it becomes clear that this upper bound is influenced by various factors such as the number of pinned nodes ℓ , the bit rate U_i allocated to each node, the coding-decoding parameters δ_i , the nonlinear boundedness conditions, the bound of control input, and the noise parameters. Obviously, when system parameters and coding-decoding parameters are fixed, the error bound is inversely related to the bit rate U_i . The influence of bit rates on synchronization performance will be analyzed in detail below.

B. Pinning Controller Design

With the help of the boundedness condition provided in Theorem 1, the desired pinning controller gains are designed in this section under the given bit rate allocation.

Theorem 2: Consider the SCNs (1), the target node (9), and the pinning controller (11) with the given positive integers U and U_i ($i \in F_0$). Then, the SED (15) is exponentially mean-square bounded if, there exist positive scalars $0 < \beta_1 < 1$, β_2 , β_3 , ε_1 , ε_2 , positive definite matrices \tilde{P}_i ($i \in F$), Q_1 , Q_2 , non-singular matrix $\mathcal{R} \triangleq \text{diag}\{R_1, R_2, \dots, R_N\}$, and matrix \mathcal{K} satisfying

$$\begin{bmatrix} \Omega_{11} & \tilde{\Omega}_{12} & \tilde{\Omega}_{13} & \Omega_{14} & \Omega_{15} \\ * & \tilde{\Omega}_{22} & 0 & 0 & 0 \\ * & * & \tilde{\Omega}_{22} & 0 & 0 \\ * & * & * & -Q_1 & 0 \\ * & * & * & * & -Q_2 \end{bmatrix} < 0 \quad (37)$$

where

$$\begin{aligned} \tilde{\Omega}_{12} &\triangleq [\tilde{\Lambda} \quad \alpha \mathcal{R} \hat{B} \quad (1 - \alpha) \mathcal{R} \hat{D} \quad -\mathcal{K} \quad -\mathcal{R}]^T, \\ \tilde{\Omega}_{13} &\triangleq [0 \quad \sigma \mathcal{R} \hat{B} \quad -\sigma \mathcal{R} \hat{D} \quad 0 \quad 0]^T, \\ \tilde{\Lambda} &\triangleq \mathcal{R} \hat{A} + \mathcal{R}(W \otimes \Gamma) + \mathcal{K}, \\ \tilde{\Omega}_{22} &\triangleq P - \mathcal{R} - \mathcal{R}^T, \quad \mathcal{K} \triangleq \mathcal{R} \tilde{K}. \end{aligned}$$

Moreover, the controller gains are obtained as follows:

$$\tilde{K} = \mathcal{R}^{-1} \mathcal{K}. \quad (38)$$

Proof 2: According to the characteristic of the positive definite matrix P , we have

$$(P - \mathcal{R})P^{-1}(P - \mathcal{R})^T \geq 0, \quad (39)$$

which implies

$$P - \mathcal{R} - \mathcal{R}^T \geq -\mathcal{R}P^{-1}\mathcal{R}^T. \quad (40)$$

It is evident from inequalities (37) and (40) that

$$\begin{bmatrix} \Omega_{11} & \tilde{\Omega}_{12} & \tilde{\Omega}_{13} & \Omega_{14} & \Omega_{15} \\ * & -\mathcal{R}P^{-1}\mathcal{R}^T & 0 & 0 & 0 \\ * & * & -\mathcal{R}P^{-1}\mathcal{R}^T & 0 & 0 \\ * & * & * & -Q_1 & 0 \\ * & * & * & * & -Q_2 \end{bmatrix} < 0. \quad (41)$$

Define a matrix as $\Psi \triangleq \text{diag}\{I, I, I, I, \mathcal{R}^{-1}, \mathcal{R}^{-1}, I, I\}$. By pre-multiplying the matrix in (41) with Ψ and post-multiplying it with Ψ^T , we can conclude that the condition (18) holds. The proof is complete.

C. Co-design of Bit Rate Allocation Strategy and Controller

By allocating the given bit rates to each admissible node i ($i \in F_0$), the corresponding pinning controller is designed in Theorem 2. Obviously, it can be inferred from (36) that, given the system parameters and the quantization region, the bit rate U_i has a large impact on the upper bound of the SED, which affects the overall control performance. The objective of this section is to further reduce the upper bound by co-designing the bit rate allocation strategy and controller gains, which can be reformulated as a minimization problem.

Corollary 1: Based on Theorem 2, when the assigned bit rate U_i ($i \in F_0$) is the variable to be designed, the optimization problem for the upper bound of the SED is transformed into the following minimization one:

$$\begin{aligned} \min \quad & \frac{\beta_2 \sum_{i=1}^{\ell} \frac{n\delta_i^2}{[\sqrt{2}U_i]^2} + \mathcal{Z}}{\beta_1 \lambda_{\min}(P)} \\ \text{s.t.} \quad & (2), (37), 0 \leq U_i \leq U \quad (i \in F_0) \end{aligned} \quad (42)$$

where $\mathcal{Z} \triangleq o^2 \lambda_{\max}(P + Q_1 + Q_2)h^2 + \text{tr}(M^T P M \Theta) + \beta_3 N L^2 \bar{l}^2$. Within this framework, the pinning controller gains are derived by $\tilde{K} = \mathcal{R}^{-1} \mathcal{K}$.

Proof 3: The proof is similar to Theorem 2 and is omitted here for space saving.

Note that the minimization problem (42) is a non-convex problem that is hard to be solved. In order to address this problem, a co-design method combining the particle swarm optimization (PSO) algorithm with the linear matrix inequality (LMI) technique will be proposed in the following.

Considering that the above minimization problem contains the constraint term $0 \leq U_i \leq U$, we transform (42) into the following form by introducing a penalty function:

$$\begin{aligned} \min \quad & \frac{\beta_2 \sum_{i=1}^{\ell} \frac{n\delta_i^2}{[\sqrt{2}U_i]^2} + \mathcal{Z}}{\beta_1 \lambda_{\min}(P)} + \eta \mathcal{J}_p(\bar{U}) \\ \text{s.t.} \quad & (37), U, U_i \in \mathbb{N} \quad (i \in F_0) \end{aligned} \quad (43)$$

where $\mathcal{J}_p(\bar{U}) \triangleq \max\{0, \sum_{i=1}^{\ell} U_i - U\}$ is the exterior penalty function with $\bar{U} \triangleq [U_1, U_2, \dots, U_{\ell}]$, and η is a constant called penalty coefficient. The fitness function of PSO algorithm is the upper bound of the SED, which is defined as

$$\mathbf{F}(\bar{U}) \triangleq \left(\beta_2 \sum_{i=1}^{\ell} \frac{n\delta_i^2}{[\sqrt{2}U_i]^2} + \mathcal{Z} \right) / (\beta_1 \lambda_{\min}(P)) + \eta \mathcal{J}_p(\bar{U}).$$

Algorithm 1: Co-design assisted by PSO Algorithm

-
- Step 1.** *Parameter initialization:* Initialize parameters \mathbf{N} , \mathbf{I} , \mathbf{w} , \mathbf{c}_1 , \mathbf{c}_2 , and the initial position \mathbf{X}_i and the initial velocity \mathbf{V}_i of each particle ($i \in \{1, 2, \dots, \mathbf{N}\}$).
- Step 2.** *Fitness update:* For each particle, update the fitness function $\mathbf{F}(\mathbf{X}_i)$ if a feasible solution for LMI (37) exists; otherwise, set the fitness function $\mathbf{F}(\mathbf{X}_i)$ as infinity.
- Step 3.** Select the particle with the minimum fitness in the population and record its position \mathbf{P}_i .
- Step 4.** *Particle swarm update:* Update the velocity and position of the particle swarm according to formulas (44) and (45), and correct it based on the boundary constraints.
- Step 5.** *Fitness function and position update:* Solve LMI (37) using the updated positions of the particles in Step 4, and obtain the updated fitness function $\mathbf{F}(\text{new}\mathbf{X}_i)$ if there is a feasible solution, otherwise, set $\mathbf{F}(\text{new}\mathbf{X}_i)$ as infinity. If $\mathbf{F}(\text{new}\mathbf{X}_i) < \mathbf{F}(\mathbf{X}_i)$, assign the value of $\mathbf{F}(\text{new}\mathbf{X}_i)$ to $\mathbf{F}(\mathbf{X}_i)$ and record updated particle's position \mathbf{P}_i .
- Step 6.** Search for particle swarm history minimum fitness and its corresponding position \mathbf{P}_g .
- Step 7.** *Bit rate allocation protocol design:* Repeat Steps 4 to 6 in a loop until the iteration is terminated. Get the particle with the minimum fitness, whose corresponding position is the optimal bit-rate allocation scheme.
- Step 8.** *Design the pinning controller:* The pinning controller's gain \tilde{K} is obtained by solving LMI (37) under optimal bit rate allocation protocol (i.e. position \mathbf{P}_g).
-

Based on the objective function described above, Algorithm 1 outlines a controller design framework that integrates PSO algorithm with the LMI technique. This algorithm aims to solve the minimization problem of the objective function with constraints and nonlinearity. In PSO, a population of particles moves through a search space to find the optimal solution. Each particle represents a potential solution characterized by its position and velocity. The particles iteratively adjust the positions based on their individual experience and information obtained from the best-performing particles in the population. In Algorithm 1, $\mathbf{X}_i \triangleq [\mathbf{X}_{i,1}, \mathbf{X}_{i,2}, \dots, \mathbf{X}_{i,\ell}]$ and $\mathbf{V}_i \triangleq [\mathbf{V}_{i,1}, \mathbf{V}_{i,2}, \dots, \mathbf{V}_{i,\ell}]$ denote the position and velocity of the i -th particle, respectively; \mathbf{N} is the number of particles in the search space, and the maximum number of iterations is represented by \mathbf{I} . The update of particle velocity and position obeys the following equations:

$$\begin{aligned} \mathbf{V}_i(\kappa + 1) = & \mathbf{w}\mathbf{V}_i(\kappa) + \mathbf{c}_1 \xi_1 (\mathbf{P}_i(\kappa) - \mathbf{X}_i(\kappa)) \\ & + \mathbf{c}_2 \xi_2 (\mathbf{P}_g(\kappa) - \mathbf{X}_i(\kappa)), \end{aligned} \quad (44)$$

$$\mathbf{X}_i(\kappa + 1) = \mathbf{X}_i(\kappa) + \mathbf{V}_i(\kappa) \quad (45)$$

where $\kappa \in \{1, 2, \dots, \mathbf{I}\}$ indicates the iteration number; w stands for the inertia weight; the acceleration constants \mathbf{c}_1 and \mathbf{c}_2 denote the self-learning factor and the group learning factor, respectively; ξ_1 and ξ_2 are two stochastic integers distributed in the interval $[1, 2]$. To prevent the particle's search position from exceeding the limited interval leading to an unproductive search, well-defined boundaries are established for both position and velocity. These boundaries, denoted as \mathbf{X}_T (upper bound), \mathbf{X}_L (lower bound) for position, as well as \mathbf{V}_T (upper bound), \mathbf{V}_L (lower bound) for velocity, serve to confine the particle's movement within a controlled and purposeful range.

By applying this algorithm, an optimal bit rate allocation strategy can be obtained, which can further advance a comprehensive analysis of different bit rates' effects on the synchronization performance of SCNs.

Remark 4: The pinning synchronization problem has been studied for a kind of SCNs in this paper. In the framework of digital communication networks, a bit-rate-constrained model has been introduced to fully reflect the constrained transmission environment. A sufficient condition guaranteeing the mean-square boundedness of the SED has been provided in Theorem 1, based on which the pinning controller's gains have been derived in Theorem 2 by allocating fixed bit rates. Furthermore, in order to optimize the synchronization performance by reducing the upper bound of the SED, a co-design of bit-rate allocation strategy and desired controller gains has been achieved in Corollary 1.

Remark 5: In comparison with the existing results regarding the pinning control for CNs, the novelties of this paper are highlighted as follows: 1) the considered pinning control strategy is new as the effects of constrained bit rates are, for the first time, discussed for SCNs with randomly occurring nonlinearities; 2) within the established theoretical framework, the relationship between the synchronization performance (in the mean-square sense) and the available bit rates is analyzed in detail; and 3) by minimizing the objective function containing the upper bound of the SED, the synchronization performance is improved through the co-design of controller gains and the bit-rate allocation protocol based on PSO algorithm.

IV. ILLUSTRATIVE EXAMPLE

In this section, a numerical simulation example is provided to verify the effectiveness of the proposed pinning controller for nonlinear SCNs under constrained bit rates.

Consider the SCNs with $N = 6$ nodes, where the first 3 nodes are selected as the pinning nodes. The system model parameters are given as follows

$$A = \begin{bmatrix} 0.7 & 0.135 \\ 0.25 & 0.61 \end{bmatrix}, B = \begin{bmatrix} 0.4 & 0.3 \\ 0.2 & 0.2 \end{bmatrix}, D = \begin{bmatrix} 0.28 & 0.3 \\ 0.3 & 0.2 \end{bmatrix}.$$

The connections among nodes are described by the coupling configuration matrix and the internal coupling matrix given as

follows:

$$W = \begin{bmatrix} -1.6 & 0.4 & 0.4 & 0.2 & 0.2 & 0.4 \\ 0 & -0.8 & 0.16 & 0.4 & 0.04 & 0.2 \\ 0.32 & 0.4 & -1.32 & 0.32 & 0.2 & 0.08 \\ 0.2 & 0.4 & 0.36 & -1.2 & 0.2 & 0.04 \\ 0.2 & 0.2 & 0.4 & 0.4 & -1.2 & 0 \\ 0.4 & 0.4 & 0.2 & 0.2 & 0.4 & -1.6 \end{bmatrix},$$

$$\Gamma = \begin{bmatrix} 0.19 & 0.1 \\ 0.4 & 0.2 \end{bmatrix}.$$

The variance of stochastic noise $\theta(s)$ is assumed to be $\Theta = 0.2I_{nN}$, and the coefficient matrices M_i ($i \in F$) are given by

$$M_1 = [0.024 \quad 0.02]^T, M_2 = [0.024 \quad 0.066]^T, \\ M_3 = [0.022 \quad 0.006]^T, M_4 = [0.046 \quad 0.002]^T, \\ M_5 = [0.03 \quad 0.02]^T, M_6 = [0.04 \quad 0.04]^T.$$

The nonlinear function $f(\cdot)$ and $g_j(\cdot)$ ($j \in \{1, 2\}$) are of the following forms:

$$f \left(\begin{bmatrix} z_1(s) \\ z_2(s) \end{bmatrix} \right) = \begin{bmatrix} 0.2 & 0.1 \\ -0.1 & 0.3 \end{bmatrix} \begin{bmatrix} z_1(s) \\ z_2(s) \end{bmatrix} + \begin{bmatrix} 0.07 \sin(s) \\ 0.1 \sin(s) \end{bmatrix}, \\ g_j(m(s)) = 0.28(|m(s) + 1| - |m(s) - 1|).$$

It can be easily verified that the above two nonlinear functions satisfy Assumptions 1 and 2, respectively. Therefore, we can obtain that

$$\chi = \begin{bmatrix} 0.2 & 0.1 \\ -0.1 & 0.3 \end{bmatrix}, \rho = 0.1, \\ \Upsilon_1 = 0, \Upsilon_2 = I_N \otimes \text{diag}\{0.56, 0.56\}.$$

Let the control input $u_0(s)$ of the target node be

$$u_0(s) = \begin{bmatrix} -0.06 & -0.09 \\ 0.1 & -0.06 \end{bmatrix} l(s).$$

Assume that the expectation of the Bernoulli random variable sequence $\gamma(s)$ is $\alpha = 0.675$, and the variance is $\sigma^2 = 0.2194$. The initial values of node $x_i(s)$ are given as follows

$$x_1(0) = [0.4 \quad 0.2]^T, x_2(0) = -[0.2 \quad 0.2]^T, \\ x_3(0) = [0.1 \quad 0.3]^T, x_4(0) = -[0.2 \quad 0.3]^T, \\ x_5(0) = -[0.4 \quad 0.5]^T, x_6(0) = [0.3 \quad -0.1]^T,$$

and the initial value of target node is chosen as $l(0) = [0 \quad 0.25]^T$.

Based on the aforementioned parameter settings, we next proceed to analyze the synchronization performance of SCNs under two different bit rate allocation protocols.

Case 1: The average allocation strategy (AAS) for bit rates refers to equitably distributing the available transmission bit rate among all permitted nodes in the SCNs to ensure that ℓ nodes receive equal transmission resources. This strategy aims to provide similar data transmission rates for ℓ nodes, thereby enhancing the synchronization performance in the network.

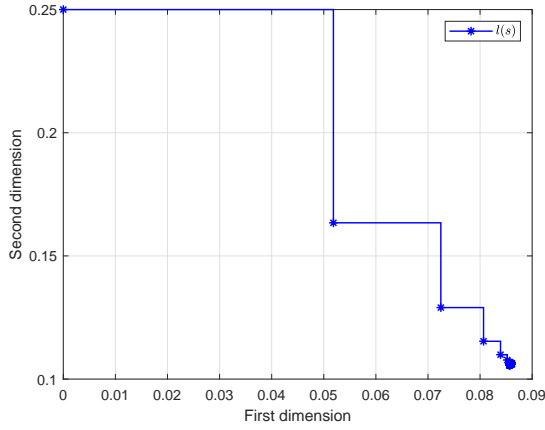


Fig. 2. The state trajectory of the target node.

For *Case 1*, we design the pinning controller with the given bit rates based on Theorem 2. Assuming that the available bit rates of the entire wireless network are $U = 32$ bps, by adopting the AAS, we have $U_1 = U_2 = U_3 = \lfloor U/3 \rfloor = 10$ bps. The parameters δ_i ($i \in F_0$) of the quantization region are chosen as $\delta_1 = \delta_2 = \delta_3 = 1$. Then, the following controller gains are obtained by solving LMI (37):

$$K_1 = \begin{bmatrix} -0.5358 & 0.2205 \\ -0.1429 & -0.2343 \end{bmatrix},$$

$$K_2 = \begin{bmatrix} -0.6171 & -0.0206 \\ -0.1648 & -0.4415 \end{bmatrix},$$

$$K_3 = \begin{bmatrix} -0.5701 & 0.1258 \\ -0.1591 & -0.3295 \end{bmatrix}.$$

By utilizing the designed pinning controller, the dynamics of SCNs is depicted in Figs. 2-5 under the above conditions. The state trajectory of the target node $l(s)$ is shown in Fig. 2, and the tracking trajectories of the SCNs nodes are displayed in Figs. 3-4. To further validate the effectiveness of the designed pinning controllers, a comparison result is presented in Fig. 5 that shows the synchronization error $e(s)$ in this work and the error $e_n(s)$ without pinning control laws.

Case 2: In certain application scenarios, the AAS for bit rates might not be the optimal strategy, as some nodes may require higher transmission speeds to perform more complex tasks as compared with other nodes. In this case, in order to improve the performance of the SCNs, it is preferred to utilize the upper bound of the SED as an indicator and employ PSO algorithm to flexibly adjust the bit rate allocation strategy. The initial values of the algorithm are given in Table I.

The superiority of the PSO-based bit rate allocation strategy as compared to AAS is exhibited as follows. Set the quantization-related parameters to be $\delta_1 = \delta_2 = \delta_3 = 1$. We consider that the totally available bits rates are 50, 32, 16 and 8 bps, and use the AAS and PSO algorithm, respectively, to evaluate the control performance and the results are listed in Table II. It can be seen from Table II that the PSO algorithm can fully utilize the available bit rates in the network, thereby

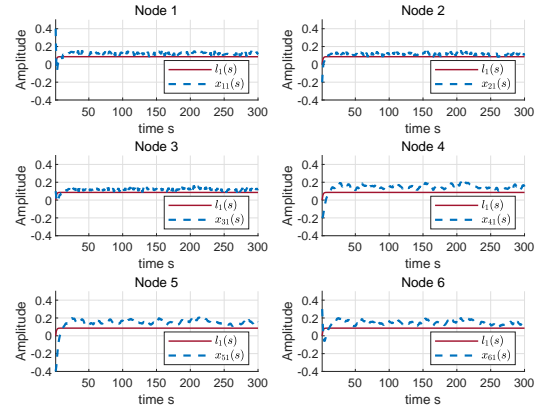


Fig. 3. Tracking trajectories in the first dimension of the nodes.

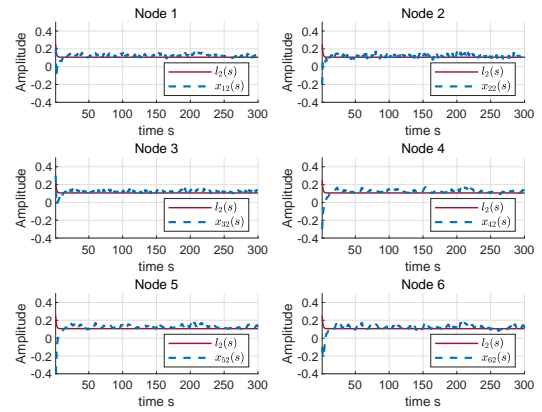


Fig. 4. Tracking trajectories in the second dimension of the nodes.

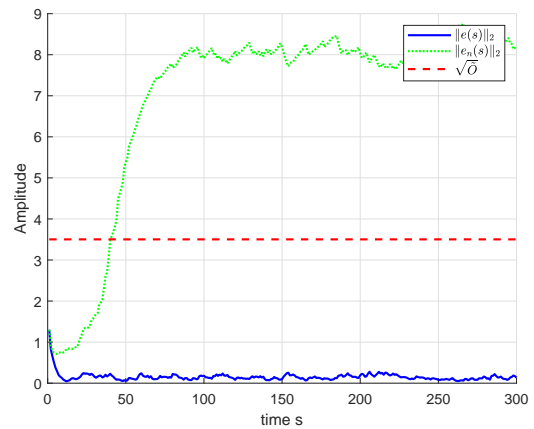


Fig. 5. Synchronization error and the AUB.

TABLE I
ALGORITHM PARAMETER INITIALIZATION

$N = 20$	$I = 30$	$\eta = 1$
$w = 1.5$	$c_1 = 1.5$	$c_2 = 1.5$
$X_T = 32$	$X_L = 1$	$V_T = 2$
$V_L = -2$	$X_i \in \mathbb{R}^3 \sim U\{1, 16\}$	$V_i \in \mathbb{R}^3 \sim U\{1, 3\}$

TABLE II
EFFECT OF DIFFERENT PROTOCOLS ON THE AUB

U (bps)	Protocol	Bit rate allocation U_1, U_2, U_3 (bps)	AUB
50	AAS	16, 16, 16	3.3661
	PSO	17, 16, 17	3.3654 (\downarrow 0.02%)
32	AAS	10, 10, 10	3.5027
	PSO	10, 11, 11	3.4576 (\downarrow 1.29%)
16	AAS	5, 5, 5	7.0958
	PSO	4, 6, 6	6.4662 (\downarrow 8.87%)
8	AAS	2, 2, 2	15.9776
	PSO	2, 2, 4	13.9389 (\downarrow 12.76%)

TABLE III
EFFECT OF DIFFERENT QUANTIZATION PARAMETERS ON THE AUB

Parameter δ_i	AUB (AAS)	AUB (PSO)
$\delta_1 = \delta_2 = \delta_3 = 3$	4.4601	4.1311
$\delta_1 = \delta_2 = \delta_3 = 1$	3.5027	3.4576
$\delta_1 = \delta_2 = \delta_3 = 0.5$	3.3991	3.3876
$\delta_1 = \delta_2 = \delta_3 = 0.25$	3.3727	3.3698

effectively reducing the AUB of SED as compared to AAS. Furthermore, it can be also concluded that as the available bit rates increase, the AUB gradually decreases. This is because, with a higher number of bit rates, the uniform quantization resolution is improved and thus the coding-decoding error is reduced.

In order to fully illustrate the impact of coding-decoding parameters on the AUB, we keep the available bit rates fixed at 32 bps and vary the quantization region δ_i . The results are shown in Table III. It is seen that for a consistent quantization level \hat{q}_i , an appropriate quantization range (approaching the absolute value of each element of $x_i(s)$) improves quantization precision. Such an improvement effectively reduces quantization errors, thereby leading to a reduction in decoding errors and subsequently lowering the AUB of the SED. Viewed from another perspective, due to the rational allocation of network bit rates by the PSO algorithm, the AUB obtained by the PSO-based approach is smaller than that achieved under the AAS.

V. CONCLUSION

In this study, we have investigated the pinning synchronization problem for SCNs under bit rate constraints. A class of SCNs with randomly occurring nonlinearities has been considered to model the complex dynamical system. The data

transmissions between node components have been achieved via bandwidth-limited channels with constrained bit rates. To accomplish synchronization between system nodes and the target node, a pinning controller has been developed in terms of the selected nodes, which is very suitable to deal with the constrained communication environment. Within the established framework, sufficient conditions have been derived to check the mean-square boundedness of the SED. By using the LMI technique, the desired pinning controller gains have been designed. Subsequently, the PSO algorithm has been introduced to facilitate the collaborative design of the pinning controller and the bit rate allocation strategy. Finally, the effectiveness of the proposed pinning control strategy has been illustrated through simulation examples, and the relationship between synchronization performance and constrained bit rates has been analyzed in detail.

It is worth noting that the phenomenon of bit-rates constraints is prevalent in networked systems. For the models involving multiple nodes transmitting information simultaneously, such as CNs, neural networks, multi-agent systems and multi-sensor systems, considering the limited bandwidth described by bit-rate constraints is of practical significance. Furthermore, it is important to consider remote state estimation, set-membership filtering, consensus problem, and similar issues within the context of this paper as a future research topic.

REFERENCES

- [1] O. Ayan, S. Hirche, A. Ephremides and W. Kellerer, Optimal finite horizon scheduling of wireless networked control systems, *IEEE/ACM Transactions on Networking*, vol. 32, no. 2, pp. 927–942, Apr. 2024.
- [2] S. Boccaletti, V. Latora, Y. Moreno, M. Chavez and D. Hwang, Complex networks: structure and dynamics, *Physics Reports*, vol. 424, pp. 175–308, Feb. 2006.
- [3] J. Chen and Q. Ling, Bit-rate conditions for the consensus of quantized multiagent systems with network-induced delays based on event triggering, *IEEE Transactions on Cybernetics*, vol. 51, no. 2, pp. 984–993, Feb. 2021.
- [4] X. Ding, J. Lu, H. Li and Y. Liu, Recent developments of Boolean networks with switching and constraints, *International Journal of Systems Science*, vol. 54, no. 14, pp. 2765–2783, 2023.
- [5] Y. Ding, M. Fu, P. Luo and F.-X. Wu, Network learning for biomarker discovery, *International Journal of Network Dynamics and Intelligence*, vol. 2, no. 1, pp. 51–65, Mar. 2023.
- [6] J. Dou and Y. Song, An improved generative adversarial network with feature filtering for imbalanced data, *International Journal of Network Dynamics and Intelligence*, vol. 2, no. 4, art. no. 100017, Dec. 2023.
- [7] Z. Hu, F. Deng and Z.-G. Wu, Synchronization of stochastic complex dynamical networks subject to consecutive packet dropouts, *IEEE Transactions on Cybernetics*, vol. 51, no. 7, pp. 3779–3788, Jul. 2021.
- [8] Y. Ju, G. Wei and W. Li, Distributed fault estimation over sensor networks: A bit rate allocation scheme, *Information Science*, vol. 633, pp. 597–612, Jul. 2023.
- [9] M. I. Khedher, H. Jmila and M. A. El-Yacoubi, On the formal evaluation of the robustness of neural networks and its pivotal relevance for AI-based safety-critical domains, *International Journal of Network Dynamics and Intelligence*, vol. 2, no. 4, art. no. 100018, Dec. 2023.
- [10] J.-Y. Li, Z. Wang, R. Lu and Y. Xu, Cluster synchronization control for discrete-time complex dynamical networks: when data transmission meets constrained bit rate, *IEEE Transactions on Neural Networks and Learning Systems*, vol. 34, no. 5, pp. 2554–2568, May 2023.
- [11] J.-Y. Li, Z. Wang, R. Lu and Y. Xu, A component-based coding-decoding approach to set-membership filtering for time-varying systems under constrained bit rate, *Automatica*, vol. 152, art. no. 110874, Mar. 2023.
- [12] N. Li, X. Wu, J. Feng and J. Lv, Fixed-time synchronization of complex dynamical networks: a novel and economical mechanism, *IEEE Transactions on Cybernetics*, vol. 52, no. 6, pp. 4430–4440, Jun. 2022.

- [13] T. Li, Z. Wang, L. Zou, B. Chen and L. Yu, A dynamic encryption-decryption scheme for replay attack detection in cyber-physical systems, *Automatica*, vol. 151, art. no. 110926, May 2023.
- [14] W. Li and F. Yang, Information fusion over network dynamics with unknown correlations: An overview, *International Journal of Network Dynamics and Intelligence*, vol. 2, no. 2, art. no. 100003, Jun. 2023.
- [15] W. Li, J. Zhou, J. Li, T. Xie and J. Lu, Cluster synchronization of two-layer networks via aperiodically intermittent pinning control, *IEEE Transactions on Circuits and Systems II: Express Briefs*, vol. 68, no. 4, pp. 1338–1342, Apr. 2021.
- [16] S. Liang, J. Liang and J. Qiu, Finite-time input-to-state stability of discrete-time stochastic switched systems: a comparison principle-based method, *International Journal of Systems Science*, vol. 54, no. 1, pp. 1–16, 2023.
- [17] N. Lin and Q. Ling, Bit-rate conditions for the consensus of quantized multiagent systems based on event triggering, *IEEE Transactions on Cybernetics*, vol. 52, no. 1, pp. 116–127, Jan. 2022.
- [18] D. Liu, Z. Wang, Y. Liu, F. E. Alsaadi and F. E. Alsaadi, Recursive state estimation for stochastic complex networks under round-robin communication protocol: handling packet disorders, *IEEE Transactions on Network Science and Engineering*, vol. 8, no. 3, pp. 2455–2468, Jul. 2021.
- [19] X. Liu, W. Tay, Z. Liu and G. Xiao, Quasi-synchronization of heterogeneous networks with a generalized Markovian topology and event-triggered communication, *IEEE Transactions on Cybernetics*, vol. 50, no. 10, pp. 4200–4213, Oct. 2020.
- [20] Y. Liu and Q. Ling, Stabilizing bit rate conditions for a scalar linear event-triggered system with Markov dropouts, *Automatica*, vol. 146, art. no. 110635, Dec. 2022.
- [21] Y. Liu, B. Shen and P. Zhang, Synchronization and state estimation for discrete-time coupled delayed complex-valued neural networks with random system parameters, *Neural Networks*, vol. 150, pp. 181–193, Jun. 2022.
- [22] Y.-C. Liu and N. Chopra, Robust controlled synchronization of interconnected robotic systems, *Proceedings of the 2010 American Control Conference*, Baltimore, MD, USA, pp. 1434–1439, Jun. 2010.
- [23] Z. Lu and G. Guo, Control and communication scheduling co-design for networked control systems: a survey, *International Journal of Systems Science*, vol. 54, no. 1, pp. 189–203, Jan. 2023.
- [24] Z. Mei and T. Oguchi, A real-time identification method of network structure in complex network systems, *International Journal of Systems Science*, vol. 54, no. 3, pp. 549–564, Feb. 2023.
- [25] Z.-H. Pang, T. Mu, F.-Y. Hou, Y. Shi and J. Sun, Two networked predictive control methods for output tracking of networked systems with plant-model mismatch, *International Journal of Systems Science*, vol. 54, no. 10, pp. 2073–2088, Jul. 2023.
- [26] D. E. Quevedo, A. Ahlen, A. S. Leong and S. Dey, On Kalman filtering over fading wireless channels with controlled transmission powers, *Automatica*, vol. 48, no. 7, pp. 1306–1316, Jul. 2012.
- [27] D. E. Quevedo, J. Ostergaard and D. Nesić, Packetized predictive control of stochastic systems over bit-rate limited channels with packet loss, *IEEE Transactions on Automatic Control*, vol. 56, no. 12, pp. 2854–2868, Dec. 2011.
- [28] A. Rajagopal and S. Chitraganti, State estimation and control for networked control systems in the presence of correlated packet drops, *International Journal of Systems Science*, vol. 54, no. 11, pp. 2352–2365, Aug. 2023.
- [29] N. F. Rulkov, Images of synchronized chaos: Experiments with circuits, *Chaos: An Interdisciplinary Journal of Nonlinear Science*, vol. 6, no. 3, pp. 262–279, Sept. 1996.
- [30] E. Sanchez and J. Perez, Input-to-state stability analysis for dynamic neural networks, *IEEE Transactions on circuits and systems I: Fundamental Theory and Applications*, vol. 46, no. 11, pp. 1395–1398, Nov. 1999.
- [31] X.-C. Shangguan, Y. He, C. Zhang, L. Jin, W. Yao, L. Jiang and M. Wu, Control performance standards-oriented event-triggered load frequency control for power systems under limited communication bandwidth, *IEEE Transactions on Control Systems Technology*, vol. 30, no. 2, pp. 860–868, Mar. 2022.
- [32] S.-H. Strogatz, Exploring complex networks, *Nature*, vol. 410, no. 6825, pp. 268–276, Mar. 2001.
- [33] X. Wan, C. Yang, C.-K. Zhang and M. Wu, Hybrid adjusting variables-dependent event-based finite-time state estimation for two-time-scale Markov jump complex networks, *IEEE Transactions on Neural Networks and Learning Systems*, vol. 35, no. 2, pp. 1487–1500, Feb. 2024.
- [34] J. Wang and X. Liu, Cluster synchronization for multi-weighted and directed complex networks via pinning control, *IEEE Transactions on Circuits and Systems II: Express Briefs*, vol. 69, no. 3, pp. 1347–1351, Mar. 2022.
- [35] L. Wang, Z. Wang, D. Zhao and G. Wei, Stabilization of linear discrete-time systems over resource-constrained networks under dynamical multiple description coding scheme, *Automatica*, vol. 156, art. no. 111160, Oct. 2023.
- [36] Y.-A. Wang, B. Shen, L. Zou and Q.-L. Han, A survey on recent advances in distributed filtering over sensor networks subject to communication constraints, *International Journal of Network Dynamics and Intelligence*, vol. 2, no. 2, art. no. 100007, Jun. 2023.
- [37] Y. Wu, H. Guo, L. Xue, N. Gunasekaran and J. Liu, Prescribed-time synchronization of stochastic complex networks with high-gain coupling, *IEEE Transactions on Circuits and Systems II: Express Briefs*, vol. 70, no. 11, pp. 4133–4137, Nov. 2023.
- [38] L. Xu and S. Ge, Exponential ultimate boundedness of nonlinear stochastic difference systems with time-varying delays, *International Journal of Control*, vol. 88, no. 5, pp. 983–989, Jan. 2015.
- [39] L. Xu and X. Liu, Prescribed-time synchronization of multiweighted and directed complex networks, *IEEE Transactions on Automatic Control*, vol. 68, no. 12, pp. 8208–8215, Dec. 2023.
- [40] Y. Xu, X. Wu, B. Mao, J. Lv and C. Xie, Fixed-time synchronization in the p -th moment for time-varying delay stochastic multilayer networks, *IEEE Transactions on Systems, Man, and Cybernetics: Systems*, vol. 52, no. 2, pp. 1135–1144, Feb. 2022.
- [41] N. Yang, X. Gu and H. Su, Synchronization for multilink stochastic complex networks via impulsive control in infinite dimensions, *IEEE Transactions on Control of Network Systems*, vol. 11, no. 2, pp. 1093–1102, Jun. 2024.
- [42] G. Zang, S. Shi and Y. Ma, Dynamic event-triggered synchronisation control for complex dynamical networks with stochastic attacks and actuator faults, *International Journal of Systems Science*, vol. 54, no. 8, pp. 1755–1773, Jun. 2023.
- [43] H. Zhang, Y. Zhou and Z. Zeng, Master-slave synchronization of neural networks with unbounded delays via adaptive method, *IEEE Transactions on Cybernetics*, vol. 53, no. 5, pp. 3277–3287, May 2023.
- [44] T. Zhang, Q. Liu, J. Liu, Z. Wang and H. Li, Multiple-bipartite consensus for networked Lagrangian systems without using neighbours’ velocity information in the directed graph, *Systems Science & Control Engineering*, vol. 11, no. 1, art. no. 2210185, Dec. 2023.
- [45] Y. Zhang, L. Zou, Y. Wang and Y.-A. Wang, Estimator design for complex networks with encoding decoding mechanism and buffer-aided strategy: a partial-nodes accessible case, *ISA transactions*, vol. 127, pp. 68–79, Aug. 2022.
- [46] L.-H. Zhao, S. Wen, C. Li, K. Shi and T. Huang, A recent survey on control for synchronization and passivity of complex networks, *IEEE Transactions on Network Science and Engineering*, vol. 9, no. 6, pp. 4235–4254, Nov. 2022.
- [47] W. Zhou, Y. Sun, X. Zhang, P. Shi, Cluster synchronization of coupled neural networks with lévy noise via event-triggered pinning control, *IEEE Transactions on Neural Networks and Learning Systems*, vol. 33, no. 11, pp. 6144–6157, Nov. 2022.
- [48] Y. Zhou, Y. Guo, C. Liu, H. Peng and H. Rao, Synchronization for Markovian master-slave neural networks: An event-triggered impulsive approach, *International Journal of Systems Science*, vol. 54, no. 12, pp. 2551–2565, Sept. 2023.
- [49] Z. Zhou, Y. Liu, J. Cao and M. Abdel-Aty, Cluster synchronization of boolean control networks with reinforcement learning, *IEEE Transactions on Circuits and Systems II: Express Briefs*, vol. 70, no. 12, pp. 4434–4438, Dec. 2023.
- [50] S. Zhu, J. Zhou and J. Lu, Estimating the region of attraction on controlled complex networks with time-varying delay, *IEEE Transactions on Automatic Control*, vol. 68, no. 1, pp. 516–523, Jun. 2023.
- [51] S. Zhu, J. Zhou, X. Yu and J. Lu, Bounded synchronization of heterogeneous complex dynamical networks: a unified approach, *IEEE Transactions on Automatic Control*, vol. 66, no. 4, pp. 1756–1762, Apr. 2021.
- [52] L. Zou, Z. Wang, J. Hu and H. Dong, Partial-node-based state estimation for delayed complex networks under intermittent measurement outliers: a multiple-order-holder approach, *IEEE Transactions on Neural Networks and Learning Systems*, vol. 34, no. 10, pp. 7181–7195, Oct. 2023.



Yuru Guo was born in Hubei province, China, in 1997. She received her B.S. degree from the school of electrical engineering, Nanjing Institute of Technology, Jiangsu, China, in 2019, majoring in Building Electricity and Intelligence. She is currently working toward the Ph.D. degree in Control Science and Engineering at Guangdong University of Technology, Guangzhou, China.

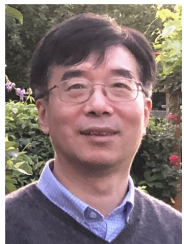
She was a Visiting Ph.D. student with the Department of Computer Science, Brunel University London, Uxbridge, U.K., from 2023 to 2024. Her

research interests include networked control systems and impulsive control.



Yong Xu (Member, IEEE) was born in Zhejiang Province, China, in 1983. He received the B.S. degree in information engineering from Nanchang Hangkong University, Nanchang, China, in 2007, the M.S. degree in control science and engineering from Hangzhou Dianzi University, Hangzhou, China, in 2010, and the Ph.D. degree in control science and engineering from Zhejiang University, Hangzhou, China, in 2014. He was a visiting internship student with the department of Electronic and Computer Engineering, Hong Kong University of Science and Technology, Hong Kong, China, from June 2013 to November 2013, where he was a Research Fellow from February 2018 to August 2018. Now he is a professor with School of Automation, at Guangdong University of Technology, Guangzhou, China.

His research interests include PID control, networked control systems, state estimation, and positive systems.



Zidong Wang (Fellow, IEEE) received the B.Sc. degree in mathematics in 1986 from Suzhou University, Suzhou, China, and the M.Sc. degree in applied mathematics in 1990 and the Ph.D. degree in electrical engineering in 1994, both from Nanjing University of Science and Technology, Nanjing, China.

He is currently a Professor of Dynamical Systems and Computing in the Department of Computer Science, Brunel University London, U.K. From 1990 to 2002, he held teaching and research appointments

in universities in China, Germany and the U.K. Prof. Wang's research interests include dynamical systems, signal processing, bioinformatics, control theory and applications. He has published a number of papers in international journals. He is a holder of the Alexander von Humboldt Research Fellowship of Germany, the JSPS Research Fellowship of Japan, William Mong Visiting Research Fellowship of Hong Kong.

Prof. Wang serves (or has served) as the Editor-in-Chief for *International Journal of Systems Science*, the Editor-in-Chief for *Neurocomputing*, the Editor-in-Chief for *Systems Science & Control Engineering*, and an Associate Editor for 12 international journals including IEEE Transactions on Automatic Control, IEEE Transactions on Control Systems Technology, IEEE Transactions on Neural Networks, IEEE Transactions on Signal Processing, and IEEE Transactions on Systems, Man, and Cybernetics-Part C. He is a Member of the Academia Europaea, a Member of the European Academy of Sciences and Arts, an Academician of the International Academy for Systems and Cybernetic Sciences, a Fellow of the IEEE, a Fellow of the Royal Statistical Society and a member of program committee for many international conferences.



Jun-Yi Li was born in Henan province, China, in 1991. He received the M.S. degree in control science and engineering from Hangzhou Dianzi University, Hangzhou, China, in 2017 and the Ph.D. degree in Control Science and Engineering from Guangdong University of Technology, Guangzhou, China, in 2021. He is currently a Lecturer with the school of Automation, Guangdong University of Technology, Guangzhou, China.

He was a visiting Ph.D. student with the Department of Computer Science, Brunel University

London, Uxbridge, U.K., from October 2019 to October 2020. His research interests include complex dynamical networks, networked systems.